# Influence of Soil Inhomogeneity on GPR for Landmine Detection

Kazunori Takahashi, Jan Igel, and Holger Preetz
Leibniz Institute for Applied Geophysics
Hannover, Germany
kazunori.takahashi@liag-hannover.de

*Abstract*—**Landmine detection by ground-penetrating radar (GPR) becomes challenging when soil is inhomogeneous. Soil inhomogeneity causes unwanted reflections (clutter) which disturb reflections from landmines. Thorough investigations on the influence of soil inhomogeneity and clutter on GPR are important for the use in demining to assess the performance and ensure the safety of the operation. In order to observe the influence of soil inhomogeneity an irrigation test was carried out and GPR data were collected after the irrigation while soil water content distribution was changing. Correlation length and variability of soil electric properties are determined by geostatistical analysis from GPR data. The theoretical calculation of Mie scattering using the determined parameters is in good agreement with power of clutter extracted from GPR data. Therefore it is demonstrated that scattering by soil inhomogeneity is governed by Mie scattering.**

***Keywords-geostatistics; landmine detection; semivariogram; scattering theory; soil inhomogeneity***

## I. INTRODUCTION

Ground-penetrating radar (GPR) has been introduced to landmine detection as stand-alone systems as well as in combination with electromagnetic induction (EMI) sensors (also known as metal detectors). The aim of using GPR is mainly discriminating landmines and metal pieces and, consequently, the demining operation is expected to be accelerated.

Electromagnetic waves are reflected when the electric properties of the propagating material change. In case of GPR permittivity of soil seems to be the greatest influential property rather than conductivity [1] and it is mainly controlled by soil water content. Inhomogeneous distribution of grain size and bulk density of soil causes a heterogeneous water content distribution which makes inhomogeneity of permittivity. Another big influence on the variance of soil moisture can come from the presence of manifold vegetation. It is the different water consumption of the plants in combination with the irregular pattern of the root system that causes a varying water uptake from the soil and thus a varying drying pattern. The resulting soil inhomogeneity further causes unwanted reflections, often referred to as clutter.

GPR has been applied to various kinds of subsurface sensing. The biggest difference between these ordinary GPR measurements and landmine detection is the measurement scale and depth range. The typical size of low metal content anti-personnel (AP) landmines is less than 10 cm in diameter and it is much smaller than objects in ordinary GPR surveys such as buried utilities and geological events. In such small scale measurements the inhomogeneity can cause a serious problem because reflections from the objects and clutter can be similar, especially if the scale of soil inhomogeneity is the same as the objects to be measured. In extreme cases clutter masks reflections from the objects, resulting in suffering the detection operation by missing mines. Therefore, it is very important to investigate the influence of soil inhomogeneity on GPR in connection to detection performance to assess effectiveness of the technique as well as the safety of demining operation. Furthermore, burial depth of deployed AP landmines is normally not deeper than 15 cm and the measurement must be focused on this rather shallow depth range. Near surface soil horizons and especially the humous topsoils are subject to a multitude of biological activities, and thus they are usually more heterogeneous than subsoil horizons. These factors sometimes make the use of GPR for landmine detection extremely difficult depending upon soil type, soil texture, land use and other external environmental conditions. Another big difference to ordinary GPR measurements is that a failure of the detection may immediately lead to a serious accident.

In this paper influence of soil inhomogeneity on GPR is discussed. The detection performance strongly depends upon appearance of clutter in the data. In order to correlate clutter and soil inhomogeneity in various conditions, an irrigation test was carried out where GPR data were collected at different degrees of inhomogeneity. Indications of soil inhomogeneity are determined from the GPR data by means of geostatistical analysis. Theoretical calculations of Mie and Rayleigh scattering with the estimated inhomogeneity are examined by comparing to clutter measured by GPR.

## II. GEOSTATISTICAL ANALYSIS

Geostatistics has been used to describe and model spatial variability of properties and has been applied to GPR measurements to describe subsurface structures (e.g., [2]-[4]). The semivariogram is a geostatistical analysis that illustrates correlation of data values in relation to the distance. The basic experimental semivariogram is described by the following equation [5]:

$$\gamma(h) = \frac{1}{2N}\sum_{i=1}^{N}\left[z(x_i + h) - z(x_i)\right]^2 \quad (1)$$

where $h$ is the lag distance, or separation distance between two data points, $z(x_i+h)$ and $z(x_i)$, and $N$ is the number of data pairs with a constant lag distance $h$ from all data points $x_i$. Typically, semivariance $\gamma(h)$ increases with lag distance $h$ up to a certain point and then it becomes constant. The lag distance $h$ and semivariance $\gamma(h)$ where $\gamma(h)$ becomes constant is called range $a$ and sill $C$, respectively. They are taken to be indications of the correlation length and variability of the data. In this study the experimental semivariogram is used to determine soil inhomogeneity from GPR data. The estimation of semivariance using (1) can be inaccurate when the data sample spacing is large and number of data pairs is small. Here a more robust estimator which implements a moving window is employed. The estimator for regularly discretized 1D data is given by the following equations [6]:

$$\gamma(h) = \gamma_0(h) + h\,\gamma_0'(h) \quad (2)$$

where $\gamma'_0(h)$ is the first derivative of $\gamma_0(h)$,

$$\gamma_0(h) = \frac{1}{n}\sum_{i=1}^{n}\left\{\frac{1}{2m}\sum_{j=1}^{h}\left[z(x_i + j) - z(x_i)\right]^2\right\}, \quad (3)$$

$n$ is the number of data values in the entire field, $m$ is the number of data values used in the inner summation. The exponential model given as [7]

$$\hat{\gamma}(h) = C\left\{1 - \exp\left[3h/a\right]\right\} \quad (4)$$

is fitted to the obtained experimental semivariograms in order to determine range $a$ and sill $C$.

Soil inhomogeneity can be defined by the correlation length and variability of the dielectric property. A change of dielectric property causes reflection (clutter) and soil inhomogeneity can therefore be determined from amplitude of GPR data. The semivariogram and the exponential model given by (2)-(4) are exploited to determine the inhomogeneity.

TABLE I. SOIL TEXTURE AND HUMUS CONTENT OF THE SOIL IN THE TEST SITE

| **Contents** | **% of mineral soil** |
|---|---|
| Clay | 1.0 |
| Silt | 6.7 |
| Sand | 92.3 |
| Humus | 6.3 [% of total soil] |

## III. EXPERIMENTAL SETUP

An irrigation test was carried out to artificially change soil water content, its distribution and the according permittivity. The experiment was conducted in a test lane build at the Leibniz Institute for Applied Geophysics (LIAG), Hannover, Germany. The soil in the test site is a natural soil material that is developed in postglacial sedimented aeolian sand. These deposits cover the quarternary sediments and form the uppermost layer in wide areas of the North German lowland plain. The texture is medium sand and the soil has a high humus content of 6.3 %. The results of the grain size analysis are given in Table I. The total pore volume (i.e., the maximum water capacity shortly after heavy rainfall or irrigation) is estimated to be about 55 %. The field capacity (i.e., the maximum water content that can be stored against gravity) is about 21 %, which corresponds to relative permittivity of 10.7. At the time of the test the lane was covered by a variety of different grasses with height of a few centimeters and the surface was relatively flat.

Approximately 12 liters per minutes of water were sprinkled around the measurement area for about 1 hour, i.e. 720 liters of water in 1 square meter area in total. An excess of water was applied to ensure that the pore system was filled up to its maximum water capacity. Relative permittivities of the soil before and immediately after the irrigation were 4 and 20.8, respectively. Since the test was carried out in summer and there had been no rainfalls more than half month prior to the test, the soil before irrigation is assumed to be in its driest natural condition.

A radar system based on a vector network analyzer (VNA) was employed and operated in frequency range of 0.5-4.0 GHz. Vivaldi antennas were used as transmitting and receiving antennas. An AP landmine mine surrogate of Type-72, whose diameter is 7.8 cm, has been in soil at a depth of 10 cm for several months and the GPR system was scanned in 1D over the target in every 2 minutes. In addition permittivity of the soil was measured at one location by a time domain reflectometry (TDR) in every half minute. The data collection was continued for approximately 18 hours after stopping irrigation. Relative permittivity after irrigation and corresponding water content obtained by Topp's equation [8] is shown in Fig. 1 and some of GPR profiles are shown in Fig. 2. 18 hours after irrigation, relative permittivity and soil water content were 11.2 and 22 %, respectively.

## IV. DATA ANALYSIS

### A. Clutter

In order to extract clutter caused by the soil inhomogeneity a region at 10-15 cm and $x < 70$ cm is selected. Maximum absolute amplitude within the region is defined as clutter amplitude at each time step. Clutter amplitude over the time after the irrigation is shown in Fig. 3.

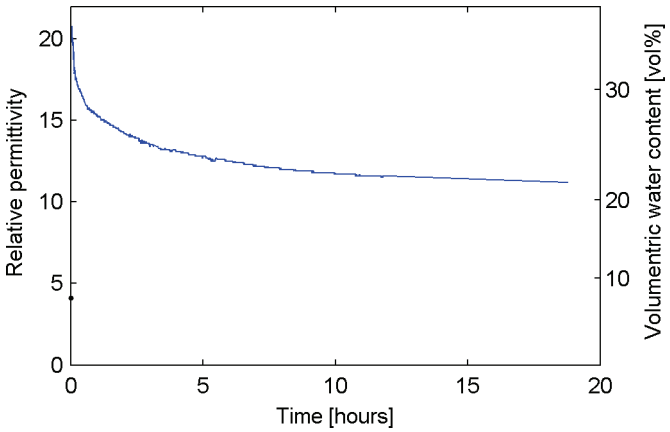


Figure 1. Relative permittivity measured by the TDR after irrigation and the corresponding water content. The dot (●) at time zero indicates relative permittivity before the irrigation.

### *B. Estimation of Inhomogeneity*

Soil inhomogeneity is estimated from the extracted clutter. Experimental semivariograms in horizontal direction are calculated from the amplitude at each depth and averaged over the depth. Some variograms are shown in Fig. 4. By fitting the exponential model given by (4), the correlation length and sill are determined as Fig. 5 in which the estimated values are plotted with respect to the time after the irrigation. The changes of the determined correlation length and variability with connection to the infiltration process of the soil could be explained as follows.

- Before irrigation, the soil was nearly completely dry that means very low water content and slightly heterogeneous pattern due to irregular drying process of soil related to vegetation and small differences in soil bulk densities. These factors may form only a low contrast in permittivity, yielding low sill and low variability in semivariogram of GPR data (Figs. 4 and 5, initial).
- When irrigation was stopped, the variability became higher but the correlation length remained at the same level as before irrigation. This may be because pattern of soil bulk density and pore distribution did not change and pores were filled with water. The higher contrast of permittivity between solid soil particles and water compared to air created higher variability (Fig. 5, at 0 hour).
- Shortly after irrigation, correlation length became longer and variability increased (0-1 hour). One of the possible explanations is that wetting of the formerly hydrophobic spaces proceeded and it led to longer correlation length but also variability increased unexpectedly. The behavior in this state is very dynamic and we do not have the exact explanation in this moment (Fig. 5, 0-5 hours after irrigation). Due to the higher variability, clutter amplitude became higher (Fig. 3).
- After 5 hours, water content already decreased to nearly the field capacity because of the high hydraulic permeability of the sandy soil (Fig. 1). In this state water distribution reflects the bulk density and grain size pattern and correlation length became the same as before irrigation. Only the medium and fine pores were still filled with water and the variability was lower than its maximum but was still higher than before irrigation (Fig. 3, 5-18 hours after irrigation).

### *C. Relationship between Clutter and Soil Inhomogeneity*

Fig. 6 shows the power of clutter plotted with respect to the correlation length relative to wavelength, defining the center frequency of 1.5 GHz. The clear tendency can be observed that there is a peak of clutter power at the relative correlation length of 1.3, although there are some outliers

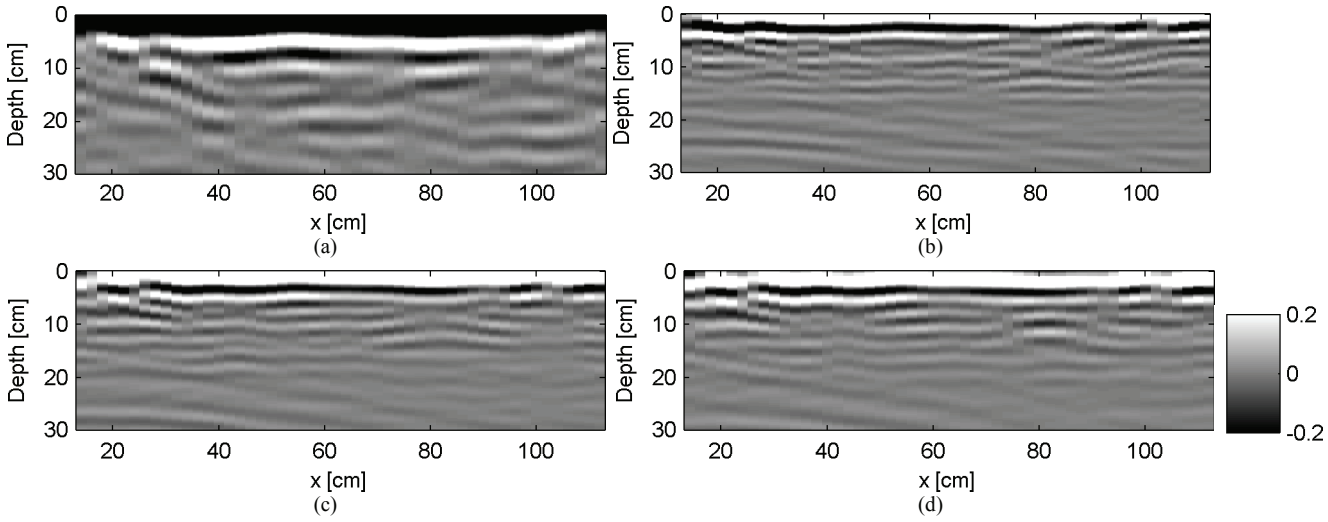


Figure 2. GPR profiles (a) before irrigation, (b) immediately after irrigation, and (c) and (d) 5and 18 hours after irrigation, respectively. Travel time is converted to depth using permittivities measured by the TDR. A Type-72 AP landmine model is buried at $x$ = 80 cm and a depth of 10 cm.

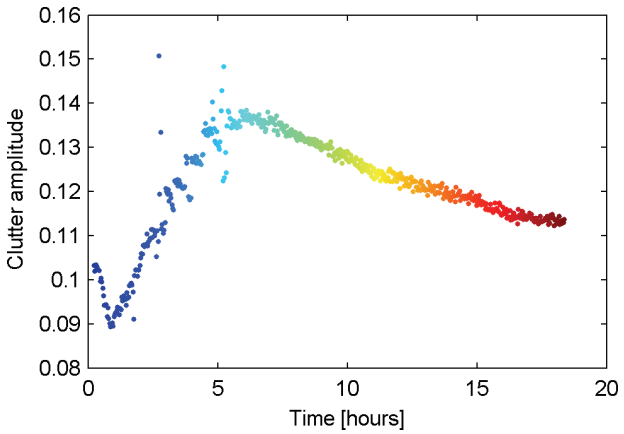


Figure 3. Variation of clutter amplitude with respect to time after irrigation. The color of dots corresponds to time after irrigation.

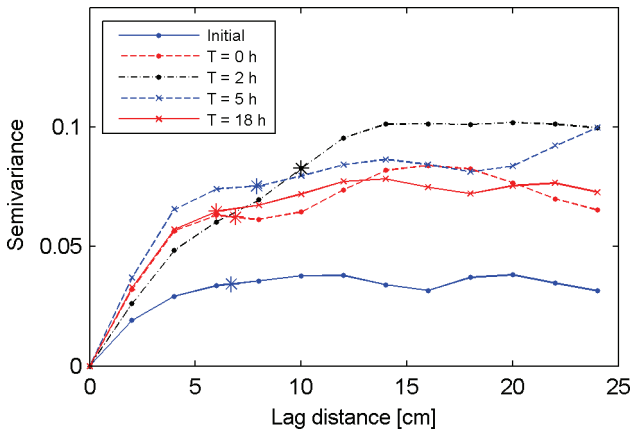


Figure 4. Experimental semivariograms before irrigation (labeled as initial), immediately after the irrigation (T = 0 h), and 2, 5 and 18 hours after the irrigation. The asterisks (*) indicate range *a* and sill *C*.

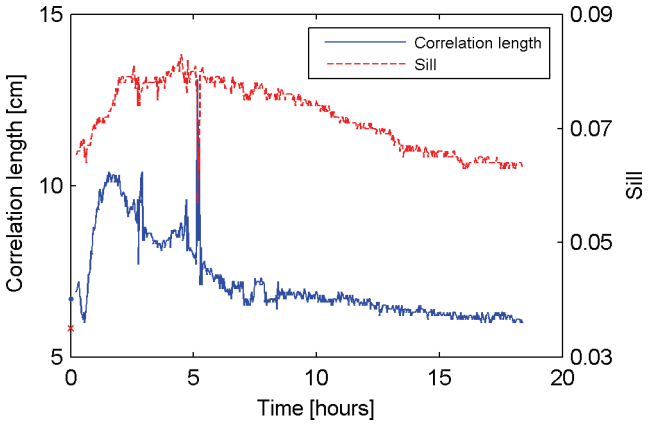


Figure 5. Determined correlation length (blue solid line) and sill (red broken line) from experimental semivariograms of the GPR data. The blue dot and red cross at time zero indicate correlation length and sill before irrigation, respectively.

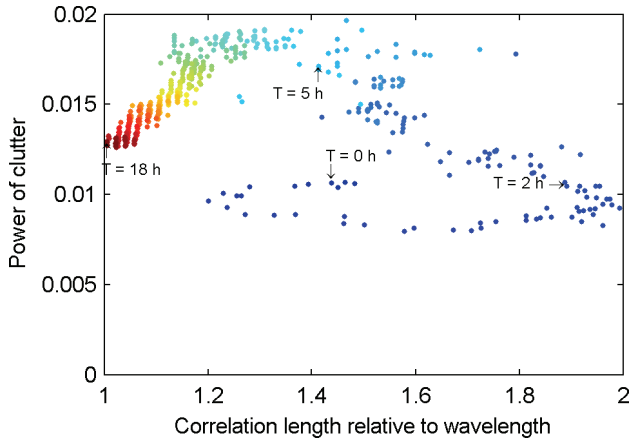


Figure 6. Power of clutter with respect to determined correlation length of the soil inhomogeneity relative to wavelength. The color of dots corresponds to time after irrigation.

observed. Fig. 7 shows the theoretical calculations of radar cross section (RCS) by the Mie solution (Fig.7a) which describes scattering by an arbitrary size of a particle and the Rayleigh approximation (Fig. 7b) which describes scattering by a small particle compared to wavelength. In the calculation a homogeneous material with the permittivity measured by TDR and a dielectric spherical particle as large as the correlation length which is determined by the semivariograms are assumed. The particle assumed to have a permittivity contrast to the surrounding medium proportional to the square root of the variance (standard deviation) determined also by the semivariograms. The experimental data (Fig. 6) is in very good agreement with the theoretical calculation by the Mie solution (Fig. 7a), especially at a range from relative correlation length of 1 to 1.3 which corresponds to times later than 6 hours after irrigation. The computation with the Rayleigh approximation (Fig. 7b), however, does not fit to the experimental data (Fig. 6), and it can therefore be confirmed that, in the range of wavelength used, the electromagnetic wave scattering caused by the soil inhomogeneity is governed by Mie scattering, rather than Rayleigh scattering. Fig. 8 shows power of clutter and RCS by the Mie solution with respect to time after irrigation. Shortly after the irrigation movement of water and changes of soil condition were very dynamic and the theoretical calculation does not fit to the experiment up to 3 hours. However, later than 3 hours, the theoretical and experimental values shows excellent agreements.

Fig. 9 shows RCS calculated by the Mie solution and the Rayleigh approximation. Refractive index of 1.18 is used, which corresponds to an ambient medium and a dielectric sphere with relative permittivities of 12 and 16.7, respectively. Up to a relative circumference of sphere of 0.5, both calculations give similar values. However, larger than 0.5, they are very different. As shown in earlier figures, correlation length relative to wavelength is ranging from 1 to 2 in our experiment. Therefore, the Rayleigh approximation is no longer applicable in this wavelength range.

The Mie solution and the Rayleigh approximation are given in Appendix.

## V. Discussions and Conclusions

Geostatistical analysis is applied to GPR data which was collected after irrigation of a dry sandy humous soil and during

the subsequent decrease of water content. The correlation length and variability of soil dielectric properties which are considered to be a measure of inhomogeneity of soil are determined from the experimental semivariograms calculated from the GPR data. By observing clutter amplitude in relation to the correlation length and variability, the scattering by soil inhomogeneity seems to be dominated by Mie scattering, rather than Rayleigh scattering. This holds true for the used center frequency of 1.5 GHz which may be common to be used for landmine detection. The theoretical calculations of the Mie solution and the Rayleigh approximation confirm our observations.

In order to correlate clutter amplitude and scattering mechanism, a very simple model is assumed for the calculation of the Mie solution in this study; a plane wave incident to a dielectric sphere embedded in a homogeneous media. In reality soil heterogeneity generally does not have such a simple shape and the sharp boundary between the sphere and the surrounding medium. Furthermore, interference between multiple spheres is not taken into account. Relatively poor fit is obtained up to 3 hours after irrigation where the correlation length is estimated to be longer. In this case the assumed model may be inappropriate; the larger correlation length indicates the gradual change of properties and the sharp boundary of the particle in the model may need to be modified. Nevertheless, the simple modeling approach describes the field data very well.

In ordinary GPR measurements for detection of utilities and subsurface structures, for instance, most of radar systems employ frequencies less than 1 GHz. In this frequency range the scattering loss due to soil inhomogeneity is often derived from the Rayleigh approximation (e.g. [9]). In the case of landmine detection higher frequency, typically higher than 1 GHz, is commonly used because relatively small objects need to be detected and only shallower depth, up to 20 cm depth, is the interest of the investigation. As a result the wavelength range of the scattering due to soil inhomogeneity is lowered to Mie scattering region and the scattered wave is observed as clutter.

Detection performance (probability of detection, POD) is often correlated to target reflection-to-clutter ratio [10]. In this study clutter amplitude can be modeled by means of the Mie solution in which permittivity measured by TDR and correlation length and variability determined by experimental semivariogram of GPR data are used as input parameters. Various modeling techniques of GPR response from landmines have been proposed (e.g. [11]). Therefore, it is possible to predict detection performance taking into account soil inhomogeneity by experimentally determining the semivariogram of soil property variations.

## APPENDIX

### THE MIE SOLUTION AND THE RAYLEIGH APPROXIMATION

RCS of a dielectric sphere with an arbitrary size embedded in a homogeneous medium is given by the Mie solution as [12]

$$\sigma_s = \frac{1}{x^2}\left|\sum_n (2n+1)(-1)^n (a_n - b_n)\right|^2 \tag{5}$$

where $x = ka$, $k$ is the wavenumber of the ambient medium and $a$ is the radius of the sphere. In case there is no change of the magnetic permeability between the dielectric sphere and the ambient medium, the coefficient $a_n$ and $b_n$ are given by

$$a_n = \frac{m^2 j_n(mx)\left[x j_n(x)\right]' - j_n(x)\left[mx j_n(mx)\right]'}{m^2 j_n(mx)\left[x h_n^{(1)}(x)\right]' - h_n^{(1)}(x)\left[mx j_n(mx)\right]'}, \tag{6a}$$

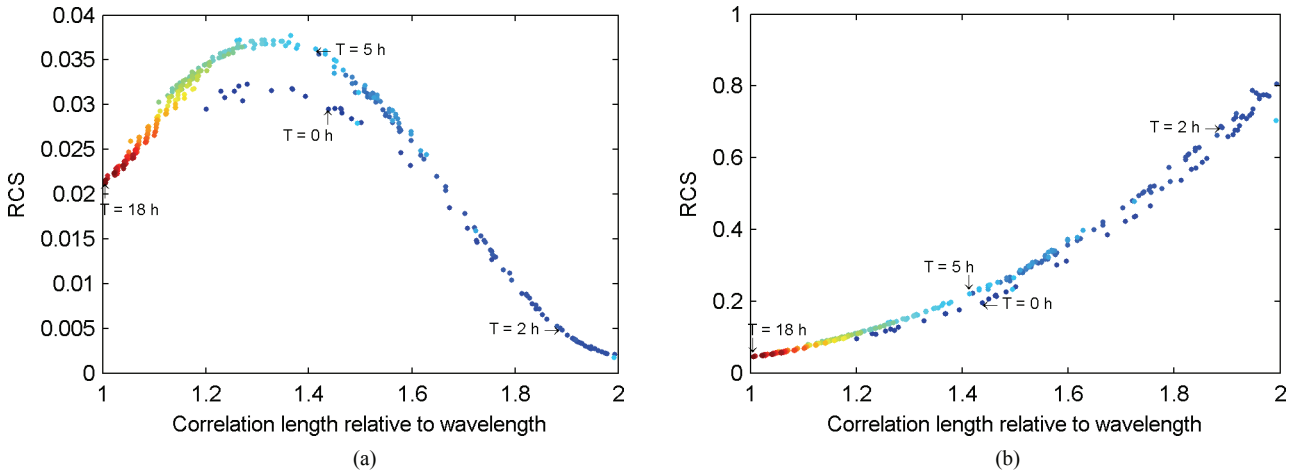


Figure 7. Radar cross section (RCS) theoritically caluclated by (a) the Mie solution and (b) the Rayleigh approximation. A dielectric sphere in a homogeneous space is assumed. Parameters needed for the calculations are obtained from the correlation length and variability which are determined by experimental semivariogram of GPR data and from TDR measurements. The color of dots corresponds to time after irrigation.

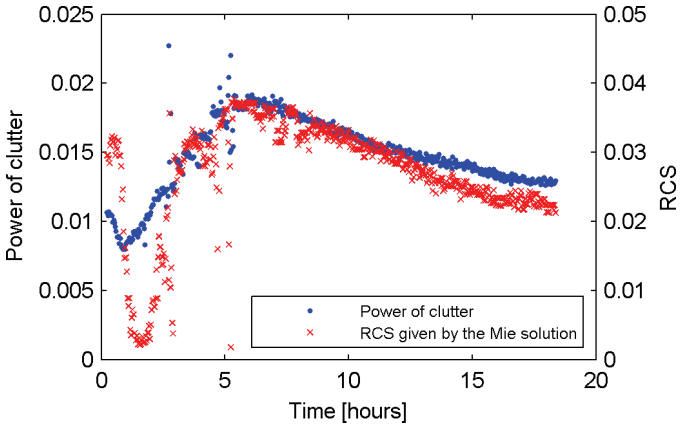


Figure 8. Power of clutter (blue dots) and RCS calculated by the Mie solution (red crosses) with respect to time after irrigation.

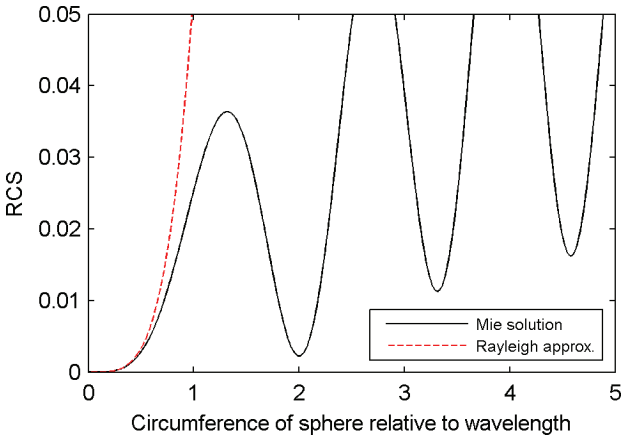


Figure 9. RCS given by the Mie solution (black solid line) and the Rayleigh approximaion (red broken line). Refractive index of 1.18 is assumed, which corresponds to a homogeneous medium and a dielectric sphere with relative permittivities of 12 and 16.7, respectively.

$$b_n = \frac{j_n(mx)\left[xj_n(x)\right]' - j_n(x)\left[mxj_n(mx)\right]'}{j_n(mx)\left[xh_n^{(1)}(x)\right]' - h_n^{(1)}(x)\left[mxj_n(mx)\right]'} \qquad (6b)$$

where $m$ denotes the refractive index and the functions $j_n(x)$ and $h_n^{(1)}(x)$ are the spherical Bessel function of first kind of order $n$ and the spherical Hankel function of order $n$, respectively. The prime means the derivative. The summation is theoretically from $n = 1$ to $\infty$, but it can be reduced up to $n_{max} = x+4x^{1/3}+2$ due to the truncation.

In case a dielectric sphere is small compared to the wavelength ($x << 1$), the Mie solution (5)-(6) can be simplified as follows and it is called the Rayleigh approximation.

$$\sigma_s = 4x^4 \left| \frac{m^2 - 1}{m^2 + 2} \right|^2 \qquad (7)$$

In the Rayleigh scattering region the scattered power of electromagnetic wave due to the particle is proportional to the inverse of the fourth power of the wavelength, whereas it is not simple when the wavelength is comparable to size of the particle or shorter.

The Rayleigh approximation describes wave scattering when the particle is much smaller than the wavelength ($x << 1$, Rayleigh region), while the Mie solution is applicable to the whole range of wavelength.

## ACKNOWLEDGMENT

The authors thank to Center for Northeast Asian Studies, Tohoku University, Japan for their support for the GPR equipment.

## REFERENCE

[1] J. Igel, "The small-scale variability of electrical soil properties − influence on GPR measurements," in proc. 12th International Conference on Ground Penetrating Radar, Birmingham, UK, June 2008.

[2] R. Knight, P. Tercier, and H. Jol, "The role of ground penetrating radar and geostatistics in reservoir description," The Leading Edge, pp. 1576-1582, Nov. 1997.

[3] J. Rea, and R. Knight, "Geostatistical analysis of ground-penetrating radar data: A means of describing spatial variation in the subsurface," Water Resour. Res., vol. 34, no. 3, pp. 392-339, Mar. 1998.

[4] P. Tercier, R. Knight, and H. Jol, "A comparison of the correlation structure in GPR images of deltaic and barrier-spit depositional environments," Geophgysics, vol. 65, no. 4, pp. 1142-1153, Jul.-Aug. 2000.

[5] C. V. Deutsch, and A. G. Journel, GSLIB Geostatistical Software Library and User's Guide, New York : Oxford Univ. Press, 1992.

[6] D. Li, and L. W. Lake, "A moving window semivariance estimator," Water Resour. Res., vol. 30, no. 5, pp. 1479-1489, 1994.

[7] E. H. Isaaks, and R. M. Srivastava, An Introduction to Applied Geostatistics, New York: Oxford Univ. Press, 1989.

[8] G. C. Topp, J. L. Davis, and A. P. Annan, "Elactromagnetic determination of soil water content: measurements in coaxial transmission lines," Water Resour. Res., vol. 16, no. 3, pp. 574-582, June 1980.

[9] H. M. Jol, Ground Penetrating Radar: Theory and Applications, Amsterdam: Elsevier, 2009.

[10] D. J. Daniels, Ground Penetrating Radat 2nd Edition, IEE Radar, Sonar and Navigation Series 15, London: IEE, 2004.

[11] F. Roth, Convolutional Models for Landmine Identification with Ground Penetrating Radar, Ph.D dissertation, Delft University of Technology, The Netherlands, 2005.

[12] C. F. Bohren, and D. Huffman, Absorption and scattering of light by small particles, New York: John Wiley, 1983.